Walking and Climbing Robot for Locomotion in 3D Environment

Hyungseok Kim, Taehun Kang and Hyoukryeol Choi
School of Mechanical Engineering, Sungkyunkwan University Chunchun-dong 300,
Jangan-gu, Suwon, Kyunggi-do, Korea, 440-746
Tel: +82-31-290-7481; Email:hrchoi@me.skku.ac.kr

Abstract: One of the traditional problems of the walking robot moving in 3D environment is how to negotiate the boundary of two plain surfaces, which may be convex or concave. In this paper the planning method in the transition region of the boundary is proposed in terms of geometrical view. In each case such as concave and convex, the trajectory that robot moves along has to be determined and the foot positions of the robot associated with the trajectory has to be estimated. The trajectory of the body is derived from the geometrical analysis of the relationship between the robot and the environment. And the position of each foot is estimated by using parameter associated with the hip and the ankle of the robot. The validity of the proposed method is demonstrated through simulations and experiments are performed in the concave and convex environments with limited slope angle.

Keywords: Walking Robot, Quadruped, Slope, MRWALLSPECT

1. INTRODUCTION

Up to now, applications of robots have been continuously discussed in the inspection of industrial utilities such as nuclear plants, oil refinery, chemical plants, buildings, bridges, etc. The tasks for the applications, in general, accompany hazardous working environments as well as difficulties in accessibility. The walking robot can be suggested as one of solutions to cope with these situations and it is required to possess the capability of traveling in three-dimensional environments, different from the general types of walking robots as shown in Fig. 1. Though the environments are composed of primitive geometrical shapes, the robot basically should be able to move such as ground to wall, wall to wall and wall to ceiling, etc. Thus the robot is strongly demanded to walk as well climb on the wall with a special adhesion tools such as suction, magnetic foot etc. and a dedicated gait planning method to move on the environment.

Many researches have been studied on this subject up to now. Hirose et al. have addressed algorithms that generate trajectories of a body and foot positions in the horizontal plain and efficient gait planning algorithm that can be applied to walking on the slope and the wall considering the effect of gravity [1-5]. Shaoping et al. have proposed the algorithm to generate free gait combined with the trajectory of the body in three-dimensional terrain [6-8]. Mohammed et al. have studied a walking algorithm and the mechanism of the robot to walk in the general terrain consisting of horizontal, inclined and vertical plain [9]. Alsalam et al. have studied transition gait from the horizontal plain to the vertical one [10]. Junmin et al. have proposed a transition gait to walk from one slope to another slope and proposed a method of estimation for the turning angle of the body [11][12].

As one of the comprehensive work for the movement in the three-dimensional environment, we propose a gait planning algorithm for the transition movement crossing the slope boundary in this paper. In this work it is addressed how to generate appropriate trajectories of the body for moving on the concave and convex slope, and the method of determining the positions of feet in accordance with the movement of the body. Simulations are carried out for hill with concave and convex boundary to prove the validity of the proposed algorithm and experiment is performed with a wall climbing robot called MRWALLSPECT III [13].

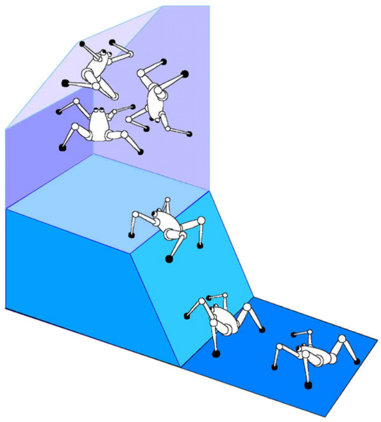

Fig. 1. Navigation in three-dimensional environment

2. MODELS OF ROBOT AND ENVIRONMENT

As depicted in Fig. 2, the leg consists of three links L_1, L_2, L_3 and passive joint ankle with yaw, pitch, roll.

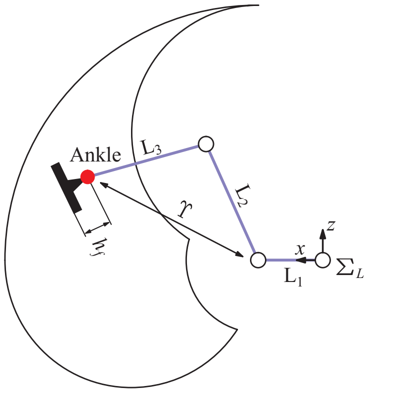

Fig. 2. Leg Structure

The height of foot is h_f and the position of foot is determined by controlling ankle position in Σ_L which is leg frame. Therefore the workspace described in Fig. 2 expresses the area that ankle can reach in *zx* plain of Σ_L. The workspace is expressed as

$$(\sqrt{x^2+y^2}-\mathrm{L}_1)^2+z^2=\Upsilon^2 \tag{1}$$

where Υ is distance between leg joint 2 and ankle and x, y and z are coordinate values of ankle in Σ_L.

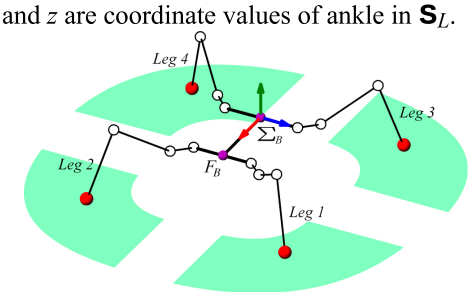

Fig. 3. Robot structure

The Fig. 3 shows robot structure that its frame Σ_B which is located in the middle of rear hip joints and the center of front body is F_B. The length of robot body is X_f and the width of front body and rear body is Y_f and Y_r respectively. The pose shown in Fig. 3 is basic form that robot repeats every gait in plain. Two parameters of the basic form, Υ of each leg and the distance h between O_B which is origin of Σ_B and plain which ankle is in contact with are utilized as reference values in transition gait. The transformation matrix from Σ_B to Σ_{Li} (i=1,2,3,4 leg number) is expressed as

$$ {}^{B}_{L1}T=\begin{bmatrix}1&0&0&X_f\\0&1&0&\frac{Y_f}{2}\\0&0&1&0\\0&0&0&1\end{bmatrix} \quad {}^{B}_{L2}T=\begin{bmatrix}1&0&0&X_f\\0&-1&0&-\frac{Y_f}{2}\\0&0&1&0\\0&0&0&1\end{bmatrix}$$
$$ {}^{B}_{L3}T=\begin{bmatrix}-1&0&0&0\\0&1&0&\frac{Y_r}{2}\\0&0&1&0\\0&0&0&1\end{bmatrix} \quad {}^{B}_{L4}T=\begin{bmatrix}-1&0&0&0\\0&-1&0&-\frac{Y_r}{2}\\0&0&1&0\\0&0&0&1\end{bmatrix} \tag{2}$$

Three-dimensional environment consists of plains which are angled each other. This is slope environment including convex, concave, wall and cliff. To simplify problem, the case that the direction of robot is perpendicular to slope boundary is considered. Let Π_{1f} be first plain that the robot is present in and Π_{2f} be second plain that robot will moves on. In transition gait, Π_{1f} and Π_{2f} are expressed as

$$\Pi_{1f}: x\sin\gamma_1 + z\cos\gamma_1 = \eta_{1f} \tag{3}$$

$$\Pi_{2f}: x\sin\gamma_2 + z\cos\gamma_2 = \eta_{2f} \tag{4}$$

where γ_1 and γ_2 are inclined angles of Π_{1f} and Π_{2f} in Σ_B respectively, η_{1f} and η_{2f} are oriented distance from Σ_B to Π_{1f} and Π_{2f} respectively. Π_{1f} and Π_{2f} are plains that the foot of robot contacts directly. As the position of foot is determined by controlling ankle position, the plain that moves parallel by foot height h_f is more useful in gait controlling. Π_1 and Π_2 are the plains that moves parallel by h_f from Π_{1f} and Π_{2f} respectively and expressed as

$$\Pi_1: x\sin\gamma_1 + z\cos\gamma_1 = \eta_1 \tag{5}$$

$$\Pi_2: x\sin\gamma_2 + z\cos\gamma_2 = \eta_2 \tag{6}$$

where η_1 and η_2 are obtained by adding η_{1f} and η_{2f} respectively.

3. GAIT ALGORITHM

In transition of slope boundary region, gait planning is constructed with two part. One is determining Σ_N which is next Σ_B after one gait and the other is determining foot positions. Σ_N is obtained by applying t_p to body trajectory and t_p is moving quantity of body. After obtaining Σ_N, foot positions can be determined by applying Υ of basic form in Σ_N. In transition of slope boundary region, foot position is not repeated in Σ_B after gait, but Υ of each leg is same in Σ_B after gait. This gives consistency to gait during transition.

3.1 Body Trajectory and Movement

Body trajectory is classified into two kind of trajectory. One is concave trajectory, the other is convex trajectory. Both concave and convex trajectories are constructed with lines and arc. Lines are determined by applying 0 to *y-axis* value in Π_{if} (i=1,2 plain number) which is moved parallel by h from Π_{ih} along *z-axis* in Σ_B. Π_{1h} and Π_{2h} are expressed as

$$\prod_{1h}: x\sin\gamma_1 + z\cos\gamma_1 = \eta_1 + h \quad (7)$$

$$\prod_{2h}: x\sin\gamma_2 + z\cos\gamma_2 = \eta_2 + h \quad (8)$$

The radius of arc is determined by γ, h, d. γ is oriented angle of slope about *y-axis* in $\mathbf{S}_B$ and d is marginal distance between ankle and boundary line of Π_1 and Π_2 when the transition gait is started or completed. The relation of γ_1, γ_2 and γ is follow:

$$\gamma = \gamma_2 - \gamma_1 \quad (9)$$

Eq. (10) and (11) describe radius R of the arc of body trajectory in concave and convex slope respectively. Fig. 4 and Fig. 5 show the body trajectory of concave and convex slope respectively. P_S is the start point of transition gait and P_E is end point of transition gait. The beginning condition of transition gait is the coincidence of F_B and P_S and the completion condition of transition is the coincidence of O_B and P_E.

$$R = \frac{d}{\tan\frac{\gamma}{2}} - h \quad (10)$$

$$R = \frac{d}{\tan\frac{\gamma}{2}} + h \quad (11)$$

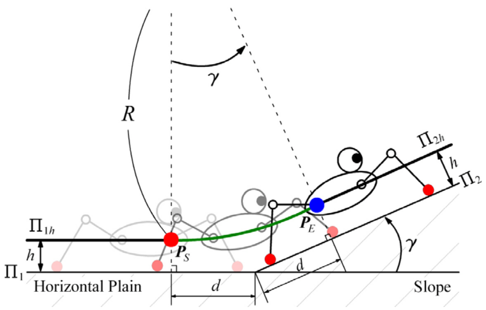

Fig. 4. Body trajectory for concave slope

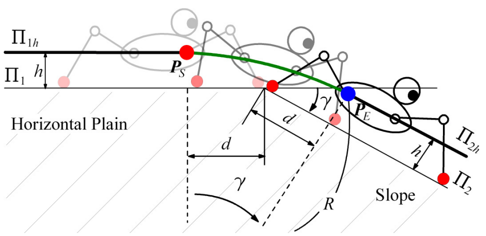

Fig. 5. Body trajectory for convex slope

In concave transition gait, situation is classified into four cases when O_B and F_B moves along body trajectory. As shown in Fig. 6, case **I** is the situation that O_B is on $\mathbf{P}_{1h}$ and F_B is on the arc. The position of O_N which is the origin of $\mathbf{S}_N$ is determined by Eq. (12). If $\|\boldsymbol{P}_S\|$ is less than t_p, P_S is O_N. F_N that is the center of front body in $\mathbf{S}_N$ is determined whether on

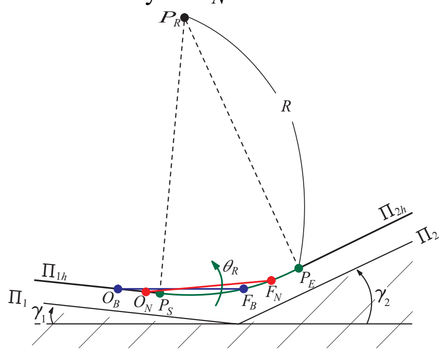

Fig. 6. Case **I** of concave transition

the arc or $\mathbf{P}_{2h}$ by comparing $\|\boldsymbol{P}_E - \boldsymbol{O}_N\|$ with X_f. When $\|\boldsymbol{P}_E - \boldsymbol{O}_N\|$ is bigger than X_f, F_N on the arc is estimated by the condition of Eq. (13) or as shown in case **II** of Fig. 7, F_N on $\mathbf{P}_{2h}$ is estimated by the condition of Eq. (14).

$$\boldsymbol{O}_N = t_p \frac{\boldsymbol{P}_S}{\|\boldsymbol{P}_S\|} \quad (12)$$

$$\begin{aligned} &\|\boldsymbol{F}_N - \boldsymbol{P}_R\| = R \\ &\|\boldsymbol{F}_N - \boldsymbol{O}_N\| = X_f \end{aligned} \quad (13)$$

$$\begin{aligned} &\boldsymbol{F}_N \cdot \mathbf{n}_{2h} = \eta_2 + h \\ &\|\boldsymbol{F}_N - \boldsymbol{O}_N\| = X_f \end{aligned} \quad (14)$$

where $\mathbf{n}_{2h}$ is normal vector of $\mathbf{P}_{2h}$, $\mathbf{n}_{2h} = [\sin\gamma_2 \quad 0 \quad \cos\gamma_2]^{\mathrm{T}}$.

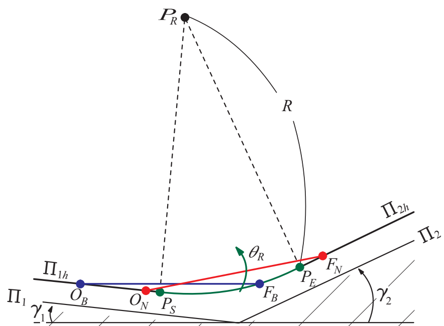

Fig. 7. Case **II** of concave transition

θ_R that is the orientation angle of $\mathbf{S}_N$ is the rotation angle about *y-axis* and estimated by Eq. (15).

$$\theta_R = \mathrm{atan2}((\boldsymbol{F}_N - \boldsymbol{O}_N)\cdot\hat{i},\ (\boldsymbol{F}_N - \boldsymbol{O}_N)\cdot\hat{k}) - \frac{\pi}{2} \quad (15)$$

where $\hat{i} = [1 \quad 0 \quad 0]^{\mathrm{T}}$ and $\hat{k} = [0 \quad 0 \quad 1]^{\mathrm{T}}$

In the case **III** and case **IV**, O_N is determined by being moved from O_B with t_p along the arc. If the arc length from O_B to P_E is less than t_p, O_N is P_E. The position vector $\boldsymbol{O}_N$ is estimated by being rotated from

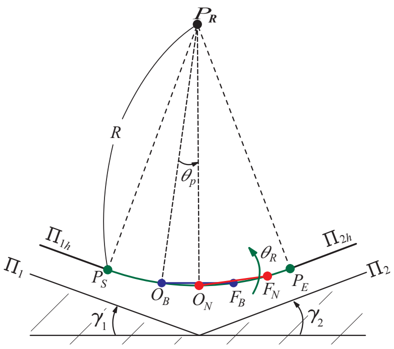

Fig. 9. Case **III** of concave transition

O_B with θ_p of Eq. (16) centering around $\boldsymbol{P}_R$ which is the position vector of P_R. The result is found in Eq. (17).

$$\theta_p = -\frac{t_p}{R} \tag{16}$$

$$\boldsymbol{O}_N = \boldsymbol{P}_R + \boldsymbol{R}_Y(\theta_p)(-\boldsymbol{P}_R) \tag{17}$$

where $\boldsymbol{R}_Y(\theta_p)$ is the rotation matrix about *y-axis*.

As θ_R is equal to θ_p in the case **III**, $\boldsymbol{F}_N$ is estimated by adding $X_f \hat{i}$ rotated by $\boldsymbol{R}_Y(\theta_p)$ to $\boldsymbol{O}_N$ as shown in Eq. (18).

$$\boldsymbol{F}_N = \boldsymbol{O}_N + X_f \cdot \boldsymbol{R}_Y(\theta_p)\hat{i} \tag{18}$$

$$\theta_R = \frac{t_p}{R} \tag{19}$$

where R is of Eq. (11)

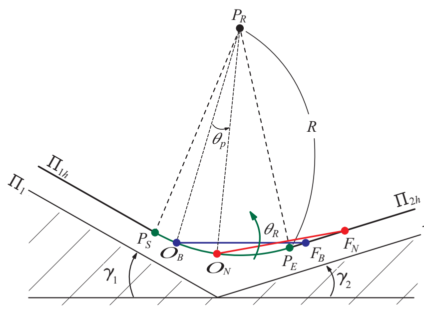

Fig. 10. Case **IV** of concave transition

In the case **IV**, $\boldsymbol{F}_N$ is found in Eq. (14) and θ_R is found in Eq. (15). In the convex transition, the case considered is only one shown in Fig. 10. O_N and F_N are determined by interior division ratio of X_f with $|\gamma_1 - \theta_R|$ and $|\gamma_2 - \theta_R|$. The interior division point P_{T2} is estimated by being moved with t_p along arc from P_{T1} which divides $\overline{O_B F_B}$ with $|\gamma_1|$ and $|\gamma_2|$ ratio interiorly. The position vector $\boldsymbol{P}_{T1}$ is $\begin{bmatrix} X_f \frac{\gamma_2}{\gamma} & 0 & 0 \end{bmatrix}^{\mathrm{T}}$ and $\boldsymbol{P}_{T2}$ is estimated by being rotated by θ_R of Eq. (19) from $\boldsymbol{P}_{T1}$ centering around $\boldsymbol{P}_R$ which is the position vector of arc center in Eq. (20). $\boldsymbol{O}_N$ and $\boldsymbol{F}_N$ are found in Eq. (21).

$$\boldsymbol{P}_{T2} = \boldsymbol{P}_R + \boldsymbol{R}_Y(\theta_R)\boldsymbol{P}_{T1} \tag{20}$$

where

$$\boldsymbol{P}_R = \boldsymbol{P}_{T1} - R\hat{k}$$

$$\boldsymbol{O}_N = \boldsymbol{P}_{T2} - \frac{|\gamma_2 - \theta_R|}{\gamma} X_f \cdot \boldsymbol{R}_Y(\theta_R)\,\hat{i}$$

$$\boldsymbol{F}_N = \boldsymbol{O}_N + X_f \cdot \boldsymbol{R}_Y(\theta_R)\,\hat{i} \tag{21}$$

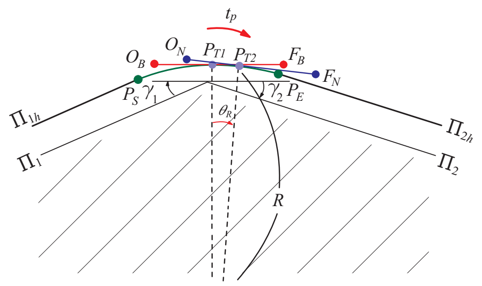

Fig. 11. Case of convex transition

In convex transition gait, the collision between the bottom of robot body and the boundary edge of convex slope must be considered. Let B_t be the distance between xy plain of $\mathbf{S}_B$ and the bottom of robot body and h_m be the distance between xy plain of robot body and the boundary edge of slope, then it is clear that h_m must be greater than B_t in order to avoid collision. The moment that h_m has minimum value is shown in Fig. 11. In this moment, $|\gamma_1|$ and $|\gamma_2|$ are equal and the workspace of each leg has to have intersected area with $\mathbf{P}_i$ (i=1 to rear legs, i=2 to front legs). h_m is found in Eq. (22) and when h is fixed, the condition is satisfied by adjusting d.

$$h_m = R - \left(\frac{d}{\tan\frac{\gamma}{2}} - h_f\right)\sqrt{1 + \frac{d^2}{r^2}} \tag{22}$$

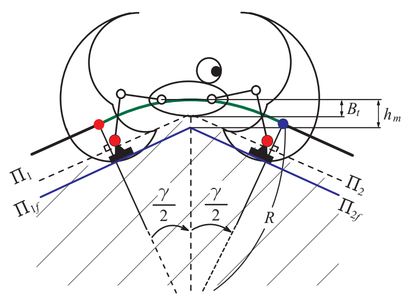

Fig. 12. Collision of convex transition

3.2 Foot Position

The foot position $\boldsymbol{P}$ on waling plain $\mathbf{P}_W$ which is inclined by γ about *y-axis* in $\mathbf{S}_L$ is determined by applying $\mathbf{U}$ of Fig. 2 in $\mathbf{S}_L$. Let $\mathbf{S}_W$ be the frame whose *xy* plain is coincident with $\mathbf{P}_W$. The origin of $\mathbf{S}_W$ is located from the origin of $\mathbf{S}_L$ by $|\eta_W|\mathbf{n}_W$ and its *y-axis* is parallel with *y-axis* of $\mathbf{S}_L$. Let ${}^W\boldsymbol{P}$ be the description of $\boldsymbol{P}$ in $\mathbf{S}_W$, then the relation of $\boldsymbol{P}$ and ${}^W\boldsymbol{P}$ is described in Eq. (23).

$$\boldsymbol{P} = {}^L_W\boldsymbol{T}\,{}^W\boldsymbol{P} \tag{23}$$

where

$${}^L_W\boldsymbol{T} = \begin{bmatrix} \boldsymbol{R}_Y(\theta_R) & |\eta_W|\mathbf{n}_W \\ 0 \;\; 0 \;\; 0 & 1 \end{bmatrix}$$

From Eq.~(1), (23) with setting ${}^W z = 0$, we have the workspace area of leg on $\mathbf{S}_W$ and the result is follow

$${}^W x^2 + {}^W y^2 + 2\mathrm{L}_1\sqrt{{}^W x\cos\gamma + \eta_W \sin\gamma} = \Upsilon^2 - \mathrm{L}_1{}^2 - \eta_W{}^2 \tag{24}$$

${}^W\boldsymbol{P}$ is determined by giving ${}^W y$ which is equal to y and $\boldsymbol{P}$ is estimated by Eq. (23).

3.3 Synthesis of Body and Foot Position

The foot position $\boldsymbol{P}$ associated with body trajectory is estimated by following steps. First, ${}^N\prod_i$ which is the description of $\mathbf{P}_i$ in $\mathbf{S}_N$ is estimated and transformed to ${}^j\prod_i$ (i=1 for j=3,4 and i=2 for j=1,2)which is description of ${}^N\prod_i$ each leg frame in Eq. (2). With applying foot position determination algorithm to ${}^j\prod_i$, ${}^j\boldsymbol{P}_j$, *j*th foot position, is determined in $\mathbf{S}_{Lj}$. By Eq. (2), ${}^N\boldsymbol{P}_j$ is estimated from ${}^j\boldsymbol{P}_j$ and finally $\boldsymbol{P}_j$ is found by transforming ${}^N\boldsymbol{P}_j$ into $\mathbf{S}_B$.

4. SIMULATION

The proposed algorithm is tested by simulation with parameters of MRWALLINSPECT III. The simulation is carried out to two case. One is the going up hill with 35 degree slope and the other is the going down the hill. In both cases, concave and convex transition gait are performed sequentially. Fig. 12 and 13 show concave and convex transition of going up hill respectively. In *Side 3* of Fig. 13, it is observed with attention whether the bottom of robot body collides with boundary edge of $\mathbf{P}_f$ which is displayed as the lower plain. Fig. 14 and 15 show convex and concave transition of going down hill respectively. Needless to say, it is observed with attention whether the bottom of robot body collides with boundary edge of $\mathbf{P}_f$ which is displayed as the lower plain in *Side 3* of Fig. 14. Consequently, the bottom of body and the boundary edge of convex slope are not collide with by applying condition of h_m in Eq. (22).

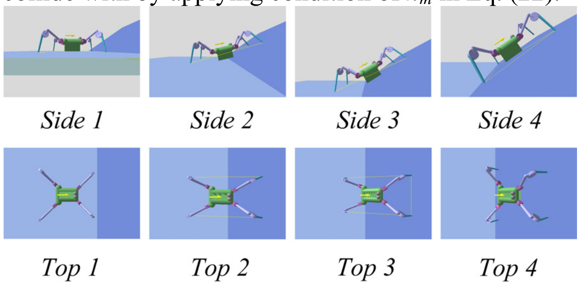

Fig. 12. Go up concave slope

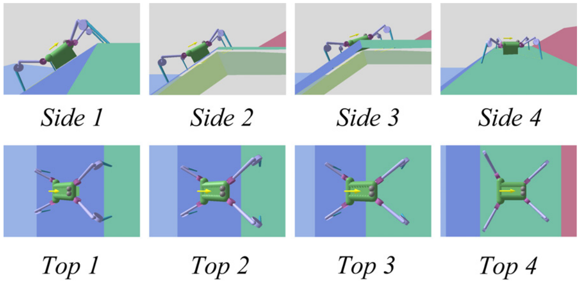

Fig. 13. Go up convex slope

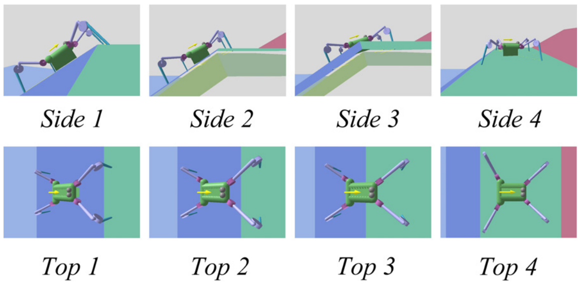

Fig. 14. Go down convex slope

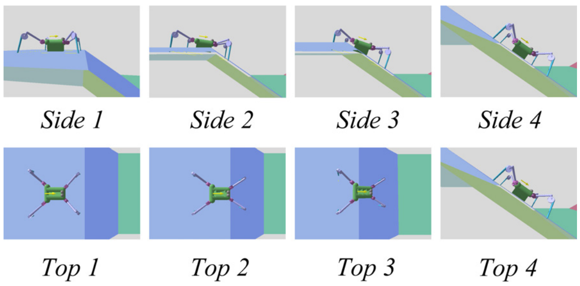

Fig. 15. Go down concave slope

5. EXPERIMENT

In this work, the validity of the proposed algorithms has been demonstrated through some experiments using a walking robot, called MRWALLSPECT III [13]. MRWALLSPECT III had been developed for walking and climbing in three dimensional unstructured environment. The climbing over a slope with concave corner was tested as shown in Fig. 16. When the robot moves up or down on the slope, tumbling of the robot and slipping of the legs should be avoided. However, in the case of the walking robot with suction pads, these problems may be neglected because the legs always have adhesive forces between the ground and the legs. The *step 1* of Fig. 16 shows the approach process for transition gait in slope environment. In this case, the

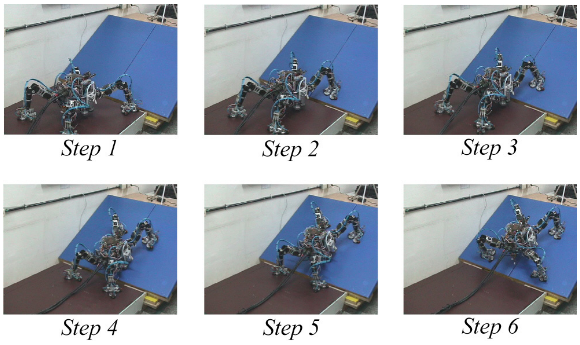

Fig. 16. Concave transition gait in 35 degrees slope

slope angle measured was an approximately 35°. And, the *step 2* and *step 3* are describe the transition in concave corner. In the last step, robot climbs the slope with plain surface using climbing gait.

6. CONCLUSION

In this paper, we proposed the transition gait algorithm for quadruped robot to negotiate boundary region between two plains. First we determine body trajectory in which robot body has to trace and suggest method to determine foot position associated with the body trajectory in terms of robot frame. Also, we explain the possibility condition of convex transition gait. The proposed algorithm is simulated successfully. And the experience with MRWALLSPECT III is tested successfully. The robot movement is smooth during gait. Our next subject is to define robot moving quantity associated with workspace of robot leg.

Acknowledgments

The authors are grateful for the support provided by a grant from the Korea Science & Engineering Foundation(KOSEF) and the Safety and Structural Integrity Research Center at the Sung Kyun Kwan University.

REFERENCES

[1] Shigeo Hirose, Hidekazu Kikuchi and Yoji Umetani, "The Standard circular gait of a quadruped walking vehicle", *Advanced Robotics*, Vol. 1, No. 2, pp. 143-164, 1986.

[2] Shigeo Hirose, Yasushi Fukuda and Hidekazu Kikuchi, "The gait control system of a quadruped walking vehicle", *Advanced Robotics*, Vol. 1, No. 4, pp. 289-323, 1986.

[3] Shigeo Hirose and Kazuhito Yokoi, "The standing posture transformation gait of a quadruped walking vehicle" *Advanced Robotics*, Vol. 2, No. 4. pp. 345-359, 1988.

[4] Keisuke Arikawa and Shigeo Hirose, "Study of Walking Robot for 3 Dimensional Terrain (optimization of walking motion based on GDA and Coupled Drive)", *Proc. of IEEE Int. Conf. on Robotics and Automation*, pp. 703-708, 1995.

[5] Hideyuki Tsukagoshi, Shigeo Hirose and Kan Yoneda, "Maneuvering Operations of the Quadruped Walking Robot on the Slope", *Proc. of IEEE/RSJ Int. Conf. on Intelligent Robots and Systems*, pp. 863-869, 1996.

[6] Shaoping Bai, K. H. Low and Teresa Zielinska, "Quadruped free gait generation combined with body trajectory planning", *Proc. of the First Workshop on Robot Motion and Control*, pp. 165-170, 1999.

[7] Shaoping Bai and K. H. Low, "Body Trajectory Generation for Legged Locomotion Systems Using A Terrain Evaluation Approach", *Proc. of IEEE Int. Conf. on Robotics and Automation*, pp. 279-2284, 2001.

[8] Shaoping Bai, K. H. Low and Teo M. Y, "Path generation of walking machines in 3D terrain", *Proc. of IEEE Int. Conf. on Robotics and Automation*, pp. 2216-2221, 2002.

[9] Mohammed Yassir Al- Zaydi and Shamsudin H. M. Amin, "Locomotion Simulation of A quadruped Robot on General Level Terrain", *Proc. of IEEE Int. Conf. on Intelligent Engineering Systems*, pp. 159-164, 1997.

[10] Abd Alsalam Sh. I. Alsalameh, Shamsudin H. M. Amin and Rosbi Mamat, "Mechanical Design of A Quadruped Robot for Horizontal Ground to Vertical Wall Movement", *Proc. of TENCON 2000*, pp. 213-217, 2000.

[11] Jummin Pan and Junshi Cheng, "Study of quadruped walking robot climbing and walking down slope", *Proc. of IEEE/RSJ Int. Conf. on Intelligent Robots and Systems*, pp. 1531-1534, 1991.

[12] Junmin Pan and Junshi Cheng, "Gait Synthesis For Quadruped Robot Walking Up and Down Slope", *Proc. of IEEE/RSJ Int. Conf. on Intelligent Robots and Systems*, pp. 532-536, 1993.

[13] Taehun Kang, Hyungseok Kim, Taeyoung Son and Hyoukryeol Choi, "Design of Quadruped Walking and Climbing Robot", *Proc. of IEEE/RSJ Intelligent Robots and Systems*, pp. 619-624, 2003.